QR code for:
Abstract LinkedIn

Sharing is encouraged

The mixed siliciclastic-carbonate sabkhas of the Late Triassic Blue Anchor Formation (Prees 2 borehole, Cheshire Basin, UK): the prelude to the End-Triassic Mass Extinction

Eleanor Frost, Stephen Hesselbo, Richard Porter, Clemens Ullman

University of Exeter, Penryn Campus,
Penryn, TR10 9FE, Cornwall, UK
Contact: ef555@exeter.ac.uk

EGU26-13721
X3.31

1: Background

Motivations

The Blue Anchor Formation represents a time period immediately prior to the earliest phase of the End-Triassic Mass Extinction (ETME). It therefore offers a unique opportunity to yield more information on the timings and causes of the ETME, and constrain timescales across and within the extinction event.

The formation has been neglected since the 1980s, and studies have largely been undertaken on outcrop sections in southwest England. Coring in the ICDP JET project (1) at Prees, Cheshire Basin, England, creates a novel opportunity to study the formation in unprecedented detail with the use of geochemical datasets.

Geological Context

The Cheshire Basin formed during Permo-Triassic rifting of the supercontinent Pangaea (2) with infill primarily controlled by fault-related subsidence of the bounding Wem-Red Rock fault system (3).

During the Late Triassic, Britain lay between 15-20 degrees North of the Equator in the northern part of the Pangaean supercontinent (4). Orbitally forced global megamonsoons affected the supercontinent in a largely semi-arid climate (5, 6), within which the red-bed sequences of the Sherwood Sandstone and Mercia Mudstone Groups were deposited.

The uppermost Mercia Mudstone contains the Blue Anchor Formation. It records a transition from ephemeral playa-lakes and saline mudflats in the underlying Branscombe Formation (6) to marginal marine muds in the overlying Westbury Formation of the Penarth Group (1, 7). The formation has classically been interpreted as deposited in supra- and intertidal sabkha environments with a sporadic link to the open sea (8, 9, 10). As such it records the widespread Rhaetic marine transgression documented across much of Europe (8, 11).

Methods

Millimetre-scale sedimentological analysis of the Prees 2C core alongside X-Ray Flouresence (XRF) analysis were used to define lithofacies, facies associations, and determine a depositional history of the formation.

Plots of XRF data against depth

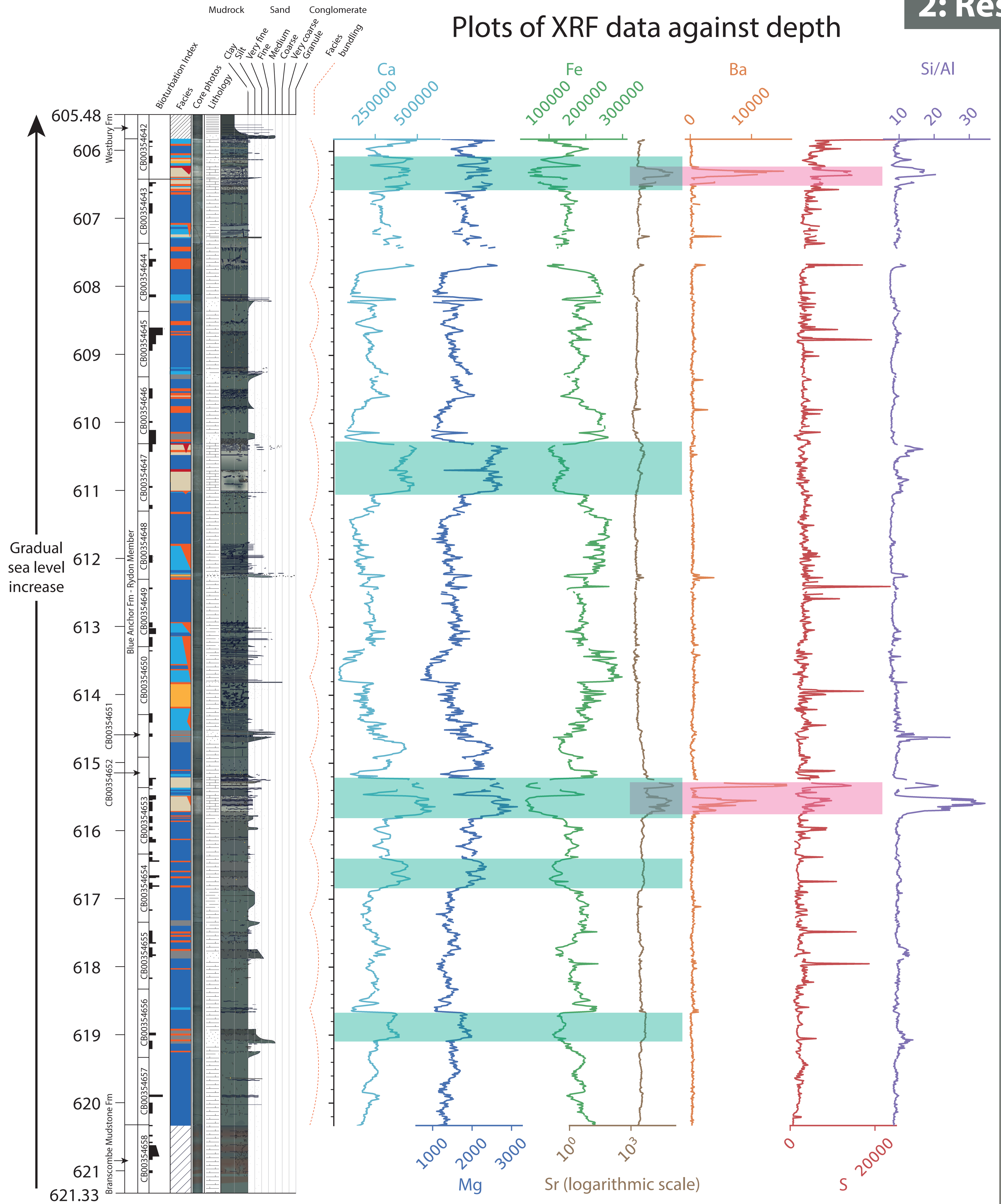

Legend

Boundaries
- Gradual, cracked boundary
- Gradual boundary
- Sharp boundary
- Erosional boundary
- Sharp uneven boundary
- Uneven wavy boundary

Lithologies
- Conglomerate
- Sandstone
- Calcareous Sandy Siltstone
- Sandy Siltstone
- Calcareous siltstone
- Siltstone

Sedimentary structures and textures
- Laminations - parallel, wavy or irregular
- Lenses of coarse material
- Lenticular bedding
- Wavy laminated bedding
- Gypsum
- Current ripples
- Wave ripples
- Pyrite nodules
- Pyrite nodules enclosed in darker material
- Mudcracks
- Brecciated appearance
- Clasts
- Clasts of laminated siltstone
- Colour mottled texture
- Dispersed sand grains
- Syn-sedimentary faults
- Teepee structures
- Rootlets/pedoturbation
- Bioturbation
- Large colour mottles

Facies
- 🟦 1: Massive Calcareous Mudstone
- 🟦 2: Laminated Calcareous Mudstone
- ⬜ 3: Silty Sandstone
- 🟨 4: Microbial Limestone
- 🟧 5: Brecciated Calcareous Mudstone
- 🟧 6: Small Cracked Bed Boundaries
- 🟥 7: Large Cracked Bed Boundaries

2: Results

Lithofacies

Core photographs

Facies Associations

1: Massive Calcareous Mudstone
Green-grey calcareous mudstone. Massive or mottled on 2 scales (mm to cm). Dispersed vf-f sand grains common. Locally bioturbation (trace fossils inc. *Taenidium*) and mm-scale nodules of pyrite (increase in abundance upwards). Generally boundaries grade into facies 6.

Interpretation: Deepest depositional environment, low energy. Perennial lakes (14, 15) below 616 mccd to subtidal lagoonal environments above.

Lacustrine/ Subaqueous

2: Laminated Calcareous Mudstone
Laminated grey to greeny-grey calcareous mudstones. Can be heavily populated with syn-sedimentary faulting ≤ 3 cm tall. Sometimes accompanying are crack networks 1-3cm tall. Locally bioturbated with trace fossils inc. *Taenidium*.

Interpretation: Deposition in quiet, subtidal lagoonal environments. Can lie behind palaeo-beach ridges, partially preserved by facies 3.

Lagoonal

3: Silty Sandstone
Very fine- to medium-grained sandstones with very high percentages of finer material. Mainly isolated beds, can have a bounding relationship with either facies 3 or 6.

Interpretation: Shallowing of water depth as shoreline progrades, depositing coarser material. Subtidal to intertidal.

Lower Intertidal/ Beach Ridges

Increasing salinity and aridity

4: Microbial Limestone
Light grey, often laminated with convoluted beds ≤ 1 cm thick and dark grey interlaminations. Highest proportions of carbonates. Teepee structures in un-convoluted beds. Upper terminations often heavily cracked (facies 7). Sometimes overprinted by rootlets or/and infilled with breccia. Boundaries within sequences may contain facies 6.

Interpretation: Upper intertidal environments where algal mats grow creating bedding. Teepee structures indicate evaporative environment.

Upper Intertidal: algal mats

5: Brecciated Calcareous Mudstone
Sequences of completely brecciated calcareous mudstone; vary significantly in appearance. Bedding indistinguishable due to complete convolution. Breccia can be composed of laminated and/or massive mudstone (facies 1 and 2).

Interpretation: Collapse breccia: cavities left after dissolution of evaporites have collapsed on themselves. Record formation of sabkhat (salt flats) in supratidal environments and later dissolution by groundwaters after burial.

Supratidal: collapse breccia

7: Large Cracked Bed Boundaries
Appearance dominated by large mudcracks > 5 cm. Larger, more angular, extending deeper than facies 6 cracks. Only occur at tops of facies 4, can be overprinted with rootlets and infilled with pedoturbated breccia.

Interpretation: Desiccation cracks formed in terrestrial hypersaline and evaporative hiatuses. Shoreline progradation causes emergence of algal mat (facies 4) to a sabkha environment, which is then desiccated. Sometimes paleosol development as an intermediary and/or later stage.

Supratidal: desiccation

6: Small Cracked Bed Boundaries
Appearance dominated by small mudcracks ≤ 1 cm in height. Create networks extending horizontally and vertically, covering upper portion of beds. Thin beds are overprinted completely to appear brecciated and cross-cut by small cracks. Within all other facies.

Interpretation: Subaqueous syneresis cracks caused by changes in salinity.

Changing salinities

Model of environmental change

The Blue Anchor Formation records a transition between the Branscombe Mudstone and the Westbury Formation, preserving three distinct environmental changes.

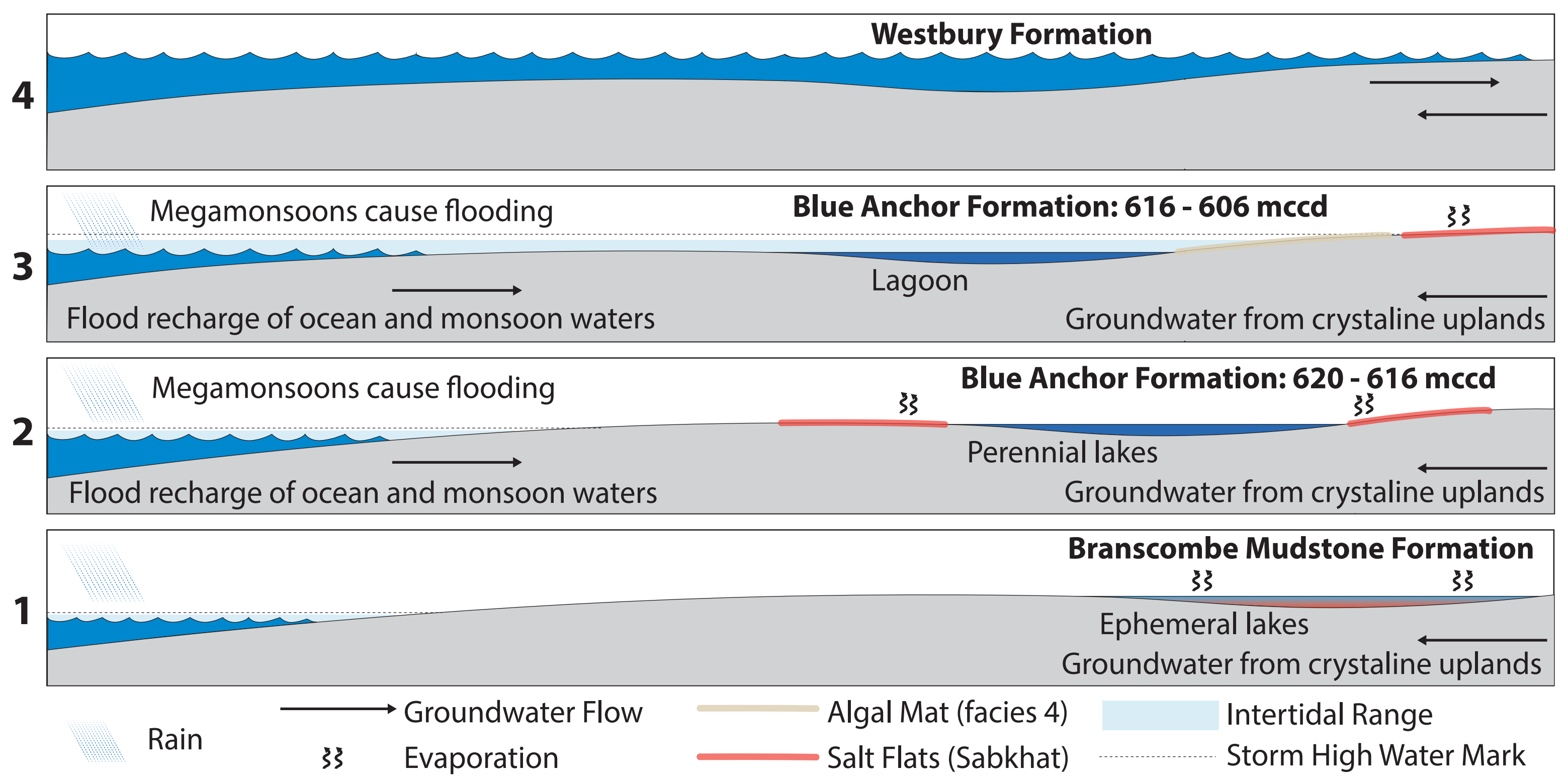

1 Branscombe Mudstone deposited in ephemeral lakes and extensive saline mudflats. Highly evaporative, hypersaline environment (6).

2 Base of Blue Anchor: sediment colour change from red to grey-blue-green. Groundwater recharges through relative sea level rise or rainfall increase; lakes become perennial. Occasional beaches.

3 616 mccd: algal mats (facies 4) indicate upper intertidal association. Relative sea level rise converts lakes to lagoons. Surrounding supratidal mudflats host sabkhas, some develop palaeosols. Arid, evaporative conditions cause desiccation (facies 7). Monsoons periodically wash away sabkha salt deposits. Occasionally floods dissolve buried salts forming collapse breccia (facies 5).

4 Abrupt sea transgression erodes uppermost Blue Anchor, deposits Westbury Formation shales above through hemipelagic settling.

Modern day analogue

Ranns of Kutch, India (16)

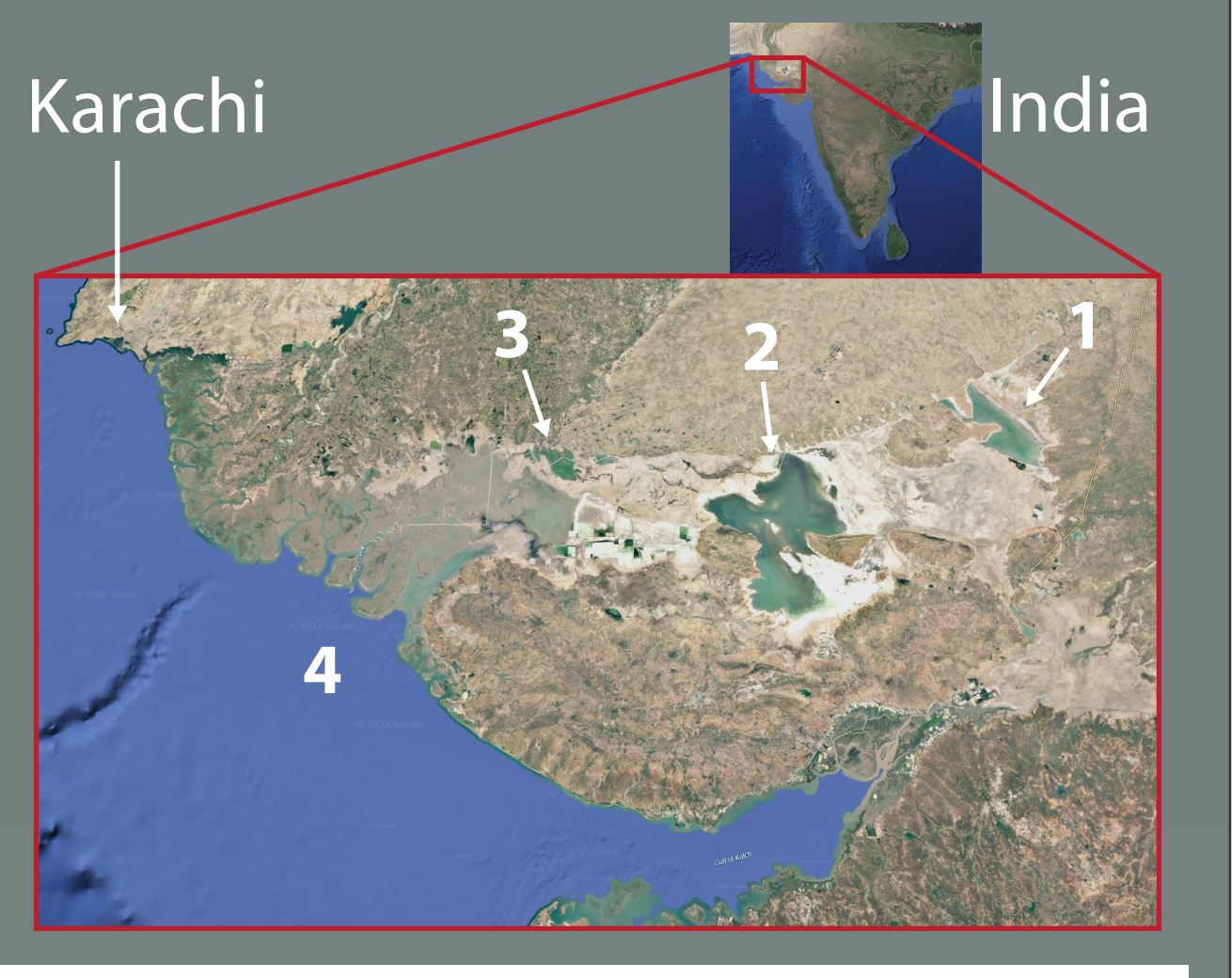

Mineralogical composition

Peaks in XRF data suggest Microbial Limestone is dominantly composed of Calcite with minor Strontianite. Although Mg and Ca covary, the Mg/Ca ratio is typically < 0.01 - much lower than the threshold for Dolomite formation (> 0.7)(12), indicating no or low Dolomite content. Troughs in Fe indicate absence of Siderite.

Peaks in XRF Sr, Ba and S counts in algal mats (facies 4) indicate displacive growth of evaporite minerals Celestine, Barite and Gypsum, as previously documented in recent sabkhas (13, 14).

Carbonate rich layers:

Calcium peaks	Calcite	✓
Magnesium peaks	High-Mg Calcite/Dolomite	?
Iron troughs	Siderite	✗
Strontium peaks	Strontianite	✓

Evaporite growth in Algal mats:

Strontium peaks	Celestine	✓
Barite peaks	Barite	✓
Sulphur peaks	Gypsum	✓

4: Conclusions and further research

7 Lithofacies are identified in the Blue Anchor Formation. Massive calcareous mudstone, laminated calcareous mudstone, silty sandstone, microbial limestone and brecciated calcareous mudstone record deposition in lacustrine, lagoonal, intertidal and supratidal environments within an overall sabkha setting. Small cracked mudstone evidences synaeresis: recurring salinity changes in either pore or surface waters throughout deposition. Large cracked mudstones evidence terrestrial hiatuses and desiccation after shoreline progradation in evaporative and hypersaline conditions.

Elemental data suggests a lack of dolomite formation in the Blue Anchor Formation Sabkha. This displays a system similar to the low-dolomite Al-Khiran sabkha (12) and unlike the classic dolomite-rich Arabian Gulf Sabkhas.

The formation records a three-phase transition from a continental to a marine system. First, groundwaters increased significantly enough, either through increased rainfall or relative sea level rise, for ephemeral lakes to become perennial. Second, relative sea level rose further, converting perennial lakes to a lagoonal system. Cyclical occurrences of subaqueous, intertidal and supratidal deposits indicate variable relative sea level. Finally, relative sea level increases dramatically, likely eroding the uppermost Blue Anchor Formation.

Further Research
Into the cyclical nature of the deposits, to assess controlling mechanisms for cyclicity.
Into the mineralogical composition of Microbial Limestone (facies 4), to determine if dolomite is present in the sabkha.

1: Hesselbo, S. P. *et al.*, (2023) *Scientific Drilling*, 32, pp. 1-25. DOI: 10.5194/sd-32-1-2023 2: Glennie, K. W., (1995) DOI: 10.1144/GSL.SP.1995.091.01.01 3: Evans, D. J., Rees, J. G., Holloway, S., (1993) DOI: 10.1144/gsjgs.150.5.0857 4: Warrington, G. and Ivimey-Cook, H.C., 1995. The Late Triassic and Early Jurassic of coastal sections in west Somerset and South and Mid-Glamorgan. 9–30 in Field Geology of the British Jurassic. London: Geological Society of London. 5: Hu, Y. *et al.*, (2023) DOI: 10.1038/s41561-023-01288-y 6: Milroy, P., Wright, V. P., Simms, M. J., (2019) DOI: 10.1111/sed.12626 7: Hounslow, M. W. and Ruffell, A. H., (2006) DOI: 10.1144/GOEWP.13 8: Mayall, M. J., (1981) DOI: 10.1017/S0016756800032246 9: Sellwood, B. W., Durkin, M. K., Kennedy, W. J., (1970) DOI: 10.1016/S0016-7878(70)80061-X 10: Warrington, G. and Whittaker, A., 1984. The Blue Anchor Formation (late Triassic) in Somerset. Proceedings of the Ussher Society, 6, pp.100-107. 11: Landon E. N. U., Duffin, C. J., Hildebrandt, C., Davies, T. G., Simms, M. J., Benton, M. J., (2017) DOI: 10.1016/j.pgeola.2017.03.005 12: Gunatilaka, A., (1991) DOI: 10.1016/0037-0738(91)90122-T 13: Mettraux, M., Homewood, P. W., Kwarteng, A. Y., Mattner, J., (2011) DOI: 10.1002/9781444392326.ch8 14: Warren, J. K. and Kendall, C. (1985) *AAPG Bulletin*, 69(6). doi: 10.1306/AD462B46-16F7-11D7-8645000102C1865D 15: Warren, J. K. (2016) 2nd edn. doi: 10.1007/978-3-319-13512-0_3 16: Glennie, K. W. and Evans, G. (1976) *Sedimentology*, 23(5), pp. 625-647. doi: 10.1111/j.1365-3091.1976.tb00098.x